Arab Gulf J. Scient. Res., Math. Phys. Sci., **A6** (3), pp. 413-428 (1988)

Minimization of Depolarized Currents of Offset Reflectors Using Multimode Pyramidal Horns

Mostafa S. Afifi

Electrical Engineering Department, College of Engineering
King Saud University, P.O. Box 800, Riyadh 11421

ABSTRACT. The current distribution on the surface of an offset parabolic reflector antenna is analized for multimode pyramidal horn feeds. The diagonal horn feed, which gives good symmetric current distribution on the reflector surface, yields high levels of depolarized fields. These are in the order of −16 dB, and form four quadrants on the surface, alternating between positive and negative polarity, around the reflector center. Adequate compensation of this depolarization is not easy. For example, the use of large percentage mix from the TM21 mode (for vertical polarization), could only reduce these depolarization current levels to −26 dB. The depolarized currents are minimized, however, by selection of the mixture ratio of specific modes in regular pyramidal horns. Depolarization levels below −40 dB (from the main polarization level) are achieved for vertical polarization (which is parallel to the offset axis of symmetry), using the fundamental TE10 mode, with small percentage mix of the TE11 mode. For horizontal polarization, the small percentage mix needed is from the TE20 mode. In this situation the depolarization level is reduced to only −34 dB. (noting that the depolarization level of the fundamental mode, alone, is −26 dB).

Introduction

The polarity of the currents induced by irradiation from the feed pattern on the reflector surface determines the polarization of its used antenna radiation for different telecommunication functions. This correspondance, between the currents on the surface of the reflector and the radiated fields, is well known from the far field direct relation, between the radiated fields and the magnetic vector potential, given by

$$\bar{E} = -\frac{\partial \bar{A}}{\partial t},$$

where the magnetic vector potential $\bar{A} = \int_S \frac{\mu \bar{K}\, ds}{4\pi R} e^{-j\beta R}$,

μ is the permeability of the medium, $\bar{K}$ is the surface current vector, S is the current carrying surface, β is the phase coefficient of propagation ($2\pi/\lambda$), λ is the wave length, t is the time and R is the far field distance. The surface currents $\bar{K}$ are derivable from the tangential magnetic fields of the feed, at the reflector surface, using the well known relation

$$\bar{K} = 2\, \hat{a}_n \times \bar{H},$$

where $\hat{a}_n$ is the unit vector normal to the reflector surface and $\bar{H}$ is the magnetic field incident from the feed irradiation at the surface of the reflector. This relation is used by Silver (1949), Afifi (1984) and others.

The directions of the magnetic fields, at the reflector surface, directly impact the polarity of the surface currents (as can be seen from the above relations). A few techniques can be used to control the orientation of the magnetic field vectors, and consequently impact the polarity of radiation. These techniques are not detailed in the open literature, and can be summarized as follows:

1. Adjustment of the mixture ratio between the magnetic and electric vector potentials of the feed excitation. This is mainly applicable to deep reflectors, where the size of the feed is small. The simplest example for this technique is the use of a Huygen source (of equal electric and magnetic moments) to feed symmetric parabolic reflectors. In this situation the depolarized currents completely disappear, as specifically illustrated by Silver (1949). Unfortionately blockage effects of the feed and its supporting structure destroy this advantage and makes it necessary to use offset reflector configurations, necessitating uptilt of the feed, to efficiently illuminate the reflector. This, however, distroys the advantage of the Huygen source effect. The separate handling of this situation is the subject of another publication.
2. Lower tilting of the feed, and special arrangements for its aperture, in order to compensate for the uptilt. This is also possible when deep reflectors (using small focal length to diameter ratio) are used. The feed design in this situation is more complex, not yet implemented, and deserves a separate study.
3. Multimoding of the feed excitation (as handled in this paper), in order to radiate compensating magnetic field levels, for elimination of the depolarized currents. This technique is adequate for deep and shallow reflectors. Shallow reflectors are predominantly used; especially as multibeam antennas, described by Afifi (1984), Chen (1980), Al-Nasser (1987), Clarricoats (1987) and Welti (1982).

Reflector Configuration

This parabolic reflector analysis assumed to have the main axis along the positive z-axis, with the vertex on the negative z-axis, at a distance equal to the focal length F from the origin (where the focal point exists, which is the location of the feed phase center). The reflector aperture, which is the wavefront of the reflected wave, is then parallel to the X−Y plane. It is assumed also that the reflector aperture is circular with a diameter D. Such a configuration is depicted in Fig. 1. The feed aperture is at the origin and pointing off the negative Z-axis, at an angle α. A point Q on the parabolic reflector surface has a radius vector $\bar{p}$ from the origin, with the unit vector $\hat{a}_n$ normal to the surface. As the radius vector $\bar{p}$ makes an angle θ' with the negative Z-axis, the unit vector $\hat{a}_n$ makes an angle $(\theta'/2)$ with the radius vector, and the same angle $(\theta'/2)$ with the horizontal axis. Also the radius vector $\bar{p}$ has a projection on the X−Y plane, making an angle ψ' with the X-axis. These definitions lead to a unit vector normal to the paraboloid surface represented by

$$\hat{a}_n = -\sin(\theta'/2)\cos\psi'\,\hat{a}_x - \sin(\theta'/2)\sin\psi'\,\hat{a}_y + \cos(\theta'/2)\,\hat{a}_z$$

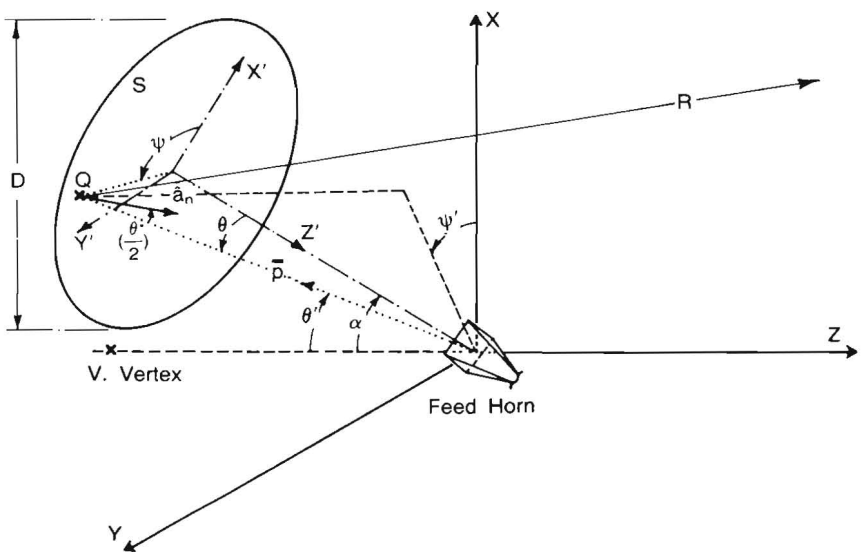

Fig. 1. Offset Reflector and Feed Configuration.

The current distribution on the reflector surface is then derived from the normal vector cross product with the magnetic field vector of the feed irradiation. This cross product is given by:

$$\bar{K} = 2(\hat{a}_n \times \bar{H}) = f(\theta',\psi') \{-\hat{a}_x[H_z \sin(\theta'/2) \sin\psi' + H_y \cos(\theta'/2)] + \hat{a}_y [H_x \cos(\theta'/2) + H_z \sin(\theta'/2) \cos\psi'] + \hat{a}_z [H_x \sin(\theta'/2) \sin\psi' - H_y \sin(\theta'/2) \cos\psi'] \} \frac{e^{-j\beta P}}{P},$$

where $\bar{H}$ is the radiated magnetic field vector from the feed, having the components H_x, H_y & H_z, and $f(\theta',\psi')$ is the radiation pattern of the feed, in the direction of the reflector.

Feed Radiation Modes

The phase center of the feed is located at the origin of the coordinate system, shown in Fig. 1, and directed to the side of the negative Z-axis, with its main axis tilted upwards at an angle α. The transformation matrix between the spherical coordinates of the feed pattern (p, θ,ψ), around its main axis, and the X′, Y′, Z′) coordinates is given by:

$$\begin{vmatrix} 0.0 & \cos\theta \cos\psi & -\sin\psi \\ 0.0 & \cos\theta \sin\psi & \cos\psi \\ 0.0 & \sin\theta & 0.0 \end{vmatrix}$$

And the transformation matrix between (X′, Y′, Z′) and the main coordinates (X, Y, Z) is given by:

$$\begin{vmatrix} \cos\alpha & 0.0 & -\sin\alpha \\ 0.0 & 1 & 0.0 \\ \sin\alpha & 0.0 & \cos\alpha \end{vmatrix}$$

The general form of the feed pattern with multimode operation is taken from Silver (1949), with minor correction of errors, generalization of polarization and gain, and use of the feed radiated magnetic fields (instead of the electric fields) yielding the following forms for the transverse electric and the transverse magnetic modes, (with summations restrictly applied to each mode, but extendable, in the computer program used, to combine both):

For the transverse electric modes

$$H_\psi = - F_g \sin\theta \sum^{m,n} P_{f\psi} \frac{K_\psi \sin(A+M) \sin(B+N)}{\beta_{c2} (A-M) (B-N)} \frac{e^{-j\beta p+u}}{p}$$

$$H_\theta = F_g \sin\theta \sin\psi_p \cos\psi_p \sum^{m,n} P_{f\theta} \frac{\sin(A+M) \sin(B+N)}{(A-M) (B-N)} \frac{e^{-j\beta p+u}}{p}$$

And for transverse magnetic modes

$$H_\psi = F_g \sin\theta \sum^{m,n} \frac{\beta}{\beta_{c2}} P_{fm} \frac{\sin(A+M) \sin(B+N)}{(A-M) (B-N)} \frac{e^{-j\beta p+u}}{p},$$

where $A = (\pi a/\lambda) \sin\theta.\cos\psi_p$, $B = (\pi b/\lambda) \sin\theta.\sin\psi_p$,

$M = (m\pi/2)$, $N = (n\pi/2)$,

F_g = is the normalized gain factor = $[(\pi^3 b)/(8\lambda^2)] \sqrt{10.2ab}$,

a = the width of the feed opening, b = its height,

$\psi_p = (\psi - \psi_{p1})$, ψ_{p1} is the polarization angle,

$P_{f\psi} = 1 + \beta_r \cos\theta + \Gamma (1 - \beta_r \cos\theta)$,

$P_{f\theta} = \cos\theta + \beta_r + \Gamma (\cos\theta - \beta_r)$,

$P_{fm} = 1 + (\cos\theta/\beta_r) + \Gamma[1 - (\cos\theta/\beta_r)]$,

$\beta_r = \beta/(2\pi/\lambda) = \sqrt{1 - (m\lambda/2a)^2 - (n\lambda/2b)^2}$,

Γ = the reflection coefficient at the feed guide,

$\beta = (2\pi/\lambda_g)$, $\beta_{c2} = (m\pi/a)^2 + (n\pi/b)^2$,

and $u = (m + n + 1) \pi/2$, with m & n defining the mode number.

(Note that these forms assume long feed horns, so that the aperture phase error effects are neglected).

These equations and their matrix transformations, as above, are programmed, in combination with the current distribution forms of the previous section, using a fast computer, with the flexibility to utilize different combinations of transverse electric and transverse magnetic modes, as needed. Individual used modes are also handled separately, as feed patterns, to identify their own performance. The utilization of these forms to minimize the depolarized performance of offset reflector antennas is developed in the following sections.

Usable Feed Modes

The well known mode of rectangular feed guides, either for propagation along the waveguide or for radiation from its aperture, is the TE10 mode. This

mode is illustrated in Fig. 2a. When this mode is combined with its identical orthogonal mode TE10, in the same opening, the diagonal horn is formed, which is well known, with its symmetric pattern performance. Such a configuration is illustrated in Fig. 2b, with 45 degrees tilt, in order to yield the same main polarity of radiation as the feed of Fig. 2a.

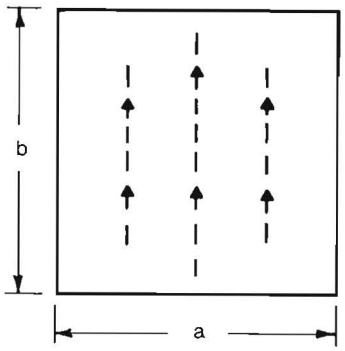

Fig. 2a. The Fundamental TE10 Mode.

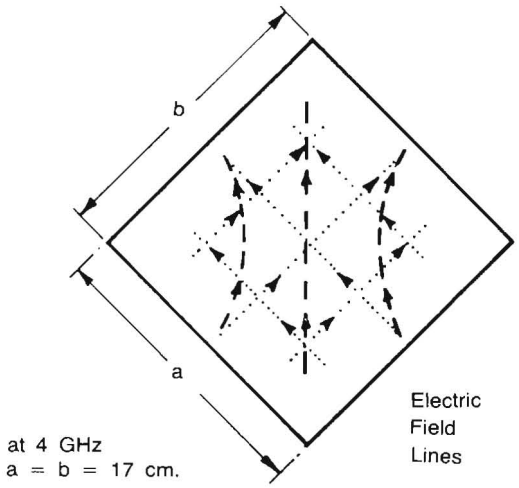

Fig. 2b. The Diagonal Horn TE10 + TE01 Modes.

These fundamental modes yield purity of polarization for the TE10 mode alone, which is evident from the straight field lines of Fig. 2a. The radiation pattern of this mode, in the 45 degree plane, which is the plane of maximum depolarization, is shown in Fig. 3a. The combined (TE10 + TE01) mode, however, of the diagonal horn of Fig. 2b, has quite curved lines, and yields high depolarization levels in the 45 degree planes, as illustrated in Fig. 3b. It can be recognized that the gain of both horns and the shape of the main polarization patterns are almost identical (in the 45 degree planes), but the depolarization levels of the diagonal horn (Fig. 3b) are almost 21 dB higher than those of the fundamental horn mode (of Fig. 3a). Note that the E− and H-plane patterns of the square horn differ widely from the symmetric patterns of the diagonal horn. This fact is well known, can be extracted from the fields of Figs. 2a & 2b, and is demonstrated by Nagi (1987). The high depolarization levels from the dual mode of the diagonal horn feed, by itself, are almost the major depolarization factors from the combined feed-offset reflector. As later shown, the depolarization lobes from the reflector system are of the same relative level, as those of the diagonal horn by itself (16 dB below the main beam level). The depolarization levels of the fundamental mode alone (Fig. 3a) is 37.5 dB below the main polarization (whereas the combined feed-offset reflector level is approximately −25 dB, as shown in the

next paragraph), meaning that this latter level is mainly due to the reflector configuration.

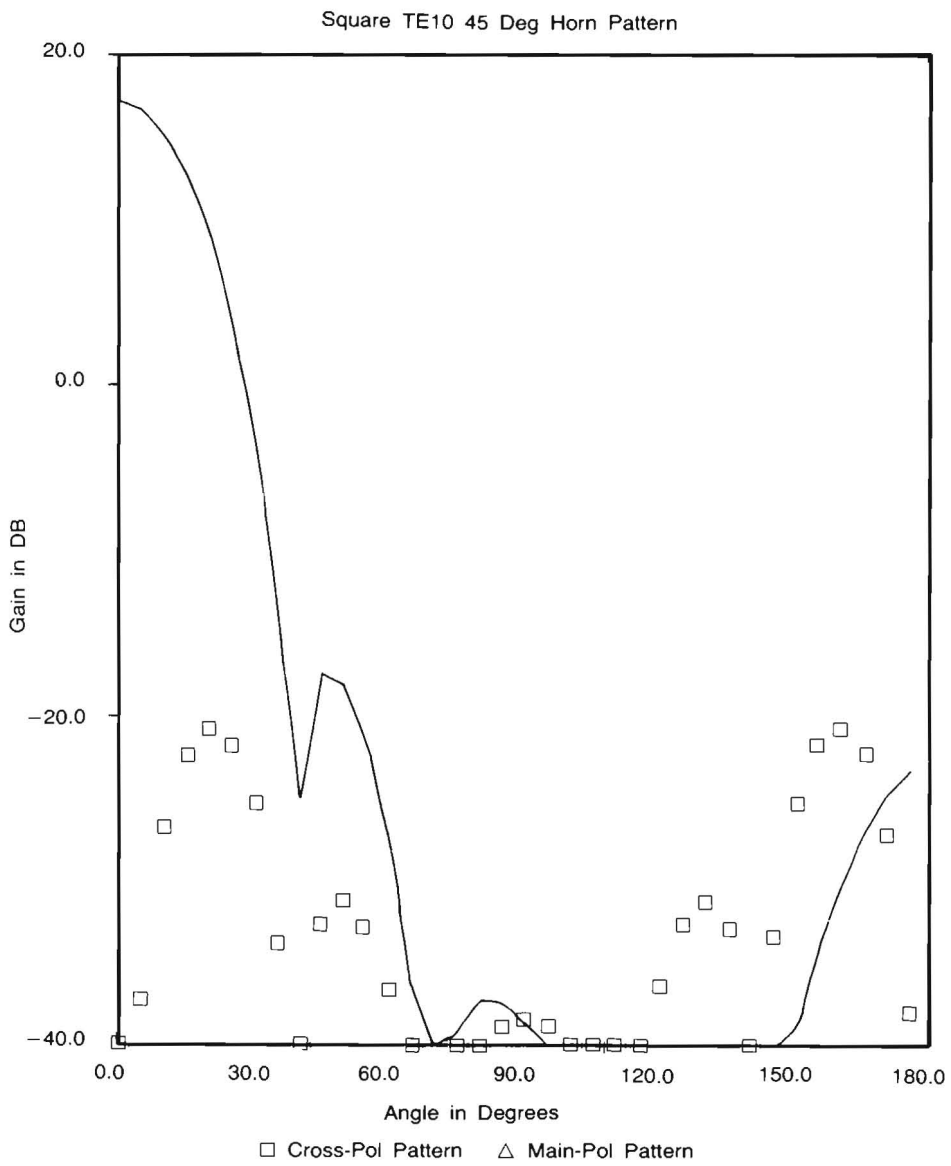

Fig. 3a. The 45° plane pattern of the pyramidal horn TE10 mode

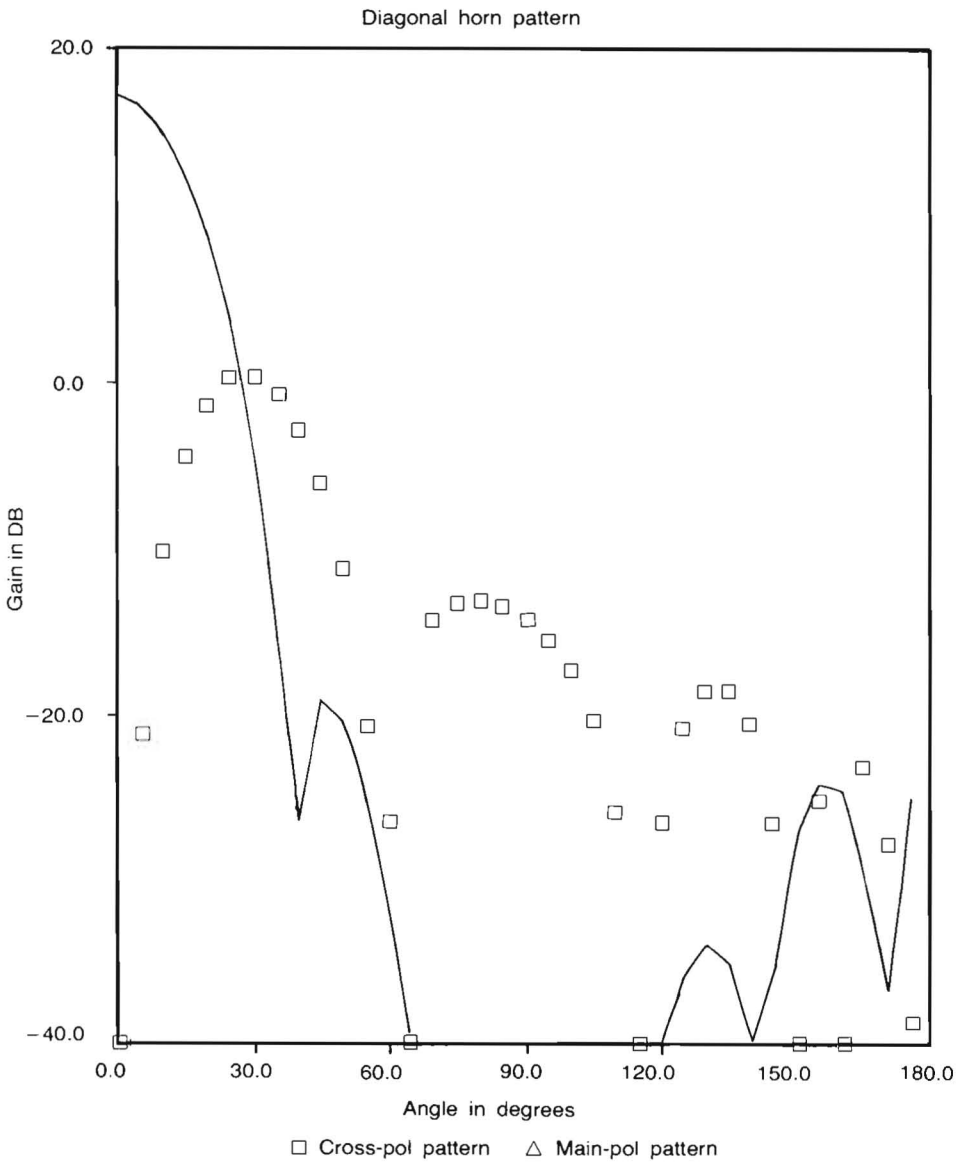

Fig. 3b. The 45° plane pattern of the diagonal horn TE10 + TE01 modes

Other usable feed modes are described in the following section, along with the reflector depolarization effects.

Reflector Interaction Effects

The offset reflector configuration used has a focal length to diameter ratio (F/D) of unity, which is the configuration of Nagi, Afifi & Samarkandi (1987) for the small earth station of the Electrical Engineering Department, of King Saud University. To clear the feed aperture from reflected waves (off the reflector surface) the lowest edge of the reflector is lifted 45 cms above the vertex. Using a diameter of 3 meters, the feed axis is needed to be tilted upwards, from the negative Z-axis, by 36 degrees, in order to point to the center of the reflector aperture. A 17 cm feed size was found to yield reasonable edge taper of illumination. The computed currents on the reflector surface, at 4 GHz, with main vertical polarization, are shown in Fig. 4a. In Fig. 4b, the depolarization pattern is shown. (In these figures three dimensional plots are used to clearly identify the performance). It can be recognized in Fig. 4a that along the axis of symmetry the edge current taper is stronger than the edge taper across the aperture. The vertical polarization is along the axis of symmetry, where the horn pattern is more directive, giving edge currents at -40 dB. The currents at the extreme edges across the aperture (in the H-plane) are only -10.5 dB, indicating asymmetry of illumination. The peak level of depolarization of Fig. 4b is 25 dB below the main polarization peak, at the center of the reflector. It is interesting to note that the

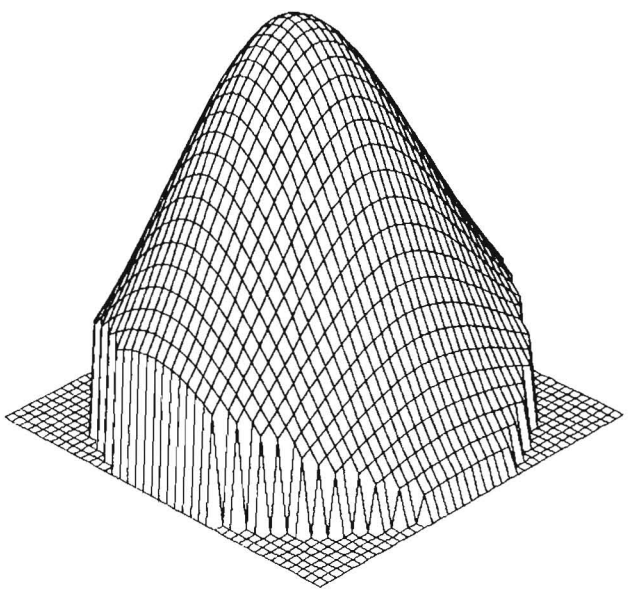

Fig. 4a. The Main Vertically Polarized Currents for the Pyramidal Horn Feed, with TE10 Mode.

integrated power of the depolarized currents (of Fig. 4b) is also 25 dB below the integrated power of the main polarized currents (of Fig. 4a). Also it is interesting to note that the shape of the depolarized pattern has equal right and left peaks with opposite polarity, *characterizing the offset reflector depolarization with dual peaks.*

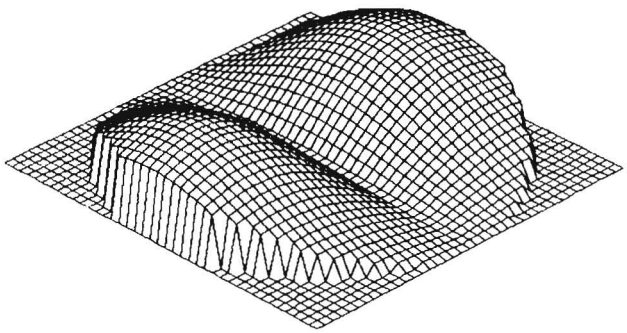

Fig. 4b. The Cross-Polarized Currents for the Pyramidal Horn, with Vertical Polarization and TE10 Mode.

When the polarization is rotated by 90 degrees the low edge illumination rotates to directions across the aperture, where the peak of depolarization exists and reduces the depolarization level to around −26 dB. This pattern is not shown here, however, as its remedy is discussed later.

In order to reduce the depolarization levels discussed above another modes are required, with excitation fields that produce opposing depolarization currents on the reflector surface. The best mode is found to be the TE20 mode, which compensates for the depolarization of the horizontally polarized currents. The TE11 mode compensates for the vertically polarized currents. Both of these modes are shown in Fig. 5. The former mode generates predominant vertically polarized waves, with opposite polarity at both sides of the reflector surface, which can be adjusted to cancel the reflector depolarization of the mainly horizontal wave. The latter mode (TE11) generates mainly horrizontally polarized currents, also with opposite polarity at both sides of the reflector, and could be adjusted to cancel the reflector depolarization of the main vertical wave. It has been found that the TE20 mode power needed is only 0.3125%; whereas the TE11 mode power needed is 0.979%. The latter is almost three times as much as the former, due to the greater purity of cancelling polarization of the former. This can be deduced from the greater curvature of the TE11 mode field lines.

The compensated depolarized pattern with vertical polarization is shown in Fig. 6. The power content of this pattern is −40 dB. The main horizontally

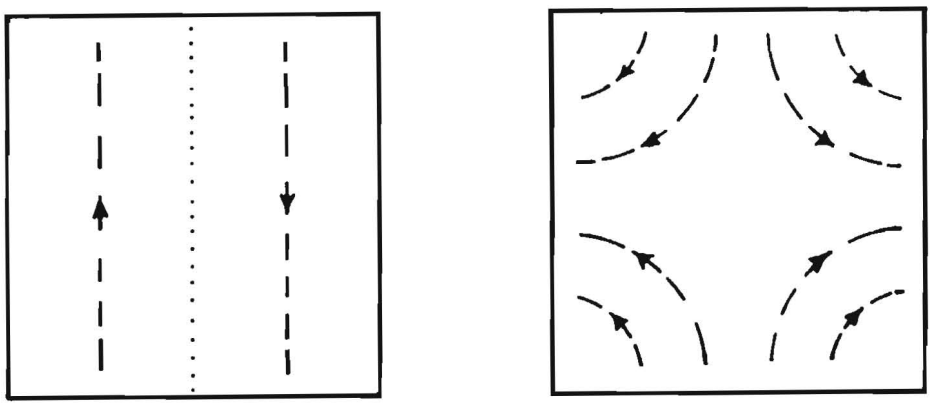

Fig. 5. Horizontal and Vertical Polarity Compensating Modes.

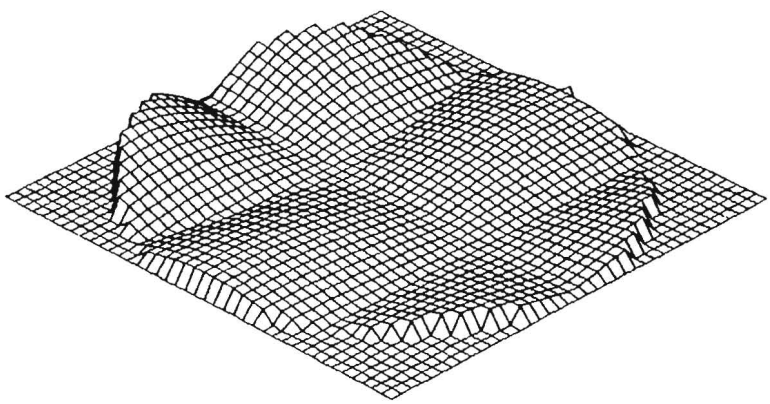

Fig. 6. The Minimized Cross-Polarized Currents, of −40 db, for a Square Horn, with Vertical Polarization.

polarized pattern is shown in Fig. 7, and the compensated depolarization, using the TE20 mode, is shown in Fig. 8. The power content of this pattern is only −34 dB. This content is higher than in the case with TE11 mode due to the impossibility of cancelling the reflector depolarization in four quadrant locations, as is the case with TE11 mode of Fig. 7.

The reflector currents generated by the diagonal horn mode are shown in Fig. 9, for the main polarization currents; and in Fig. 10, for the depolarized currents. The symmetry of illumination for the main currents is recognizable in this situation (as can be seen in Fig. 9). The power content of the depolarization of Fig. 10 is

only −16 dB (from the total power content), and correlates very well with the relative levels of the feed depolarized pattern of Fig. 3b. The mode which could reduce this level is the TM21 mode. The reduced level pattern is shown in Fig. 11. The depolarization content of this pattern is −26 dB, using a TM21 mode power content of 80%. The excitation of this mode is needed to be diagonal across the horn, which would be practically difficult to realize.

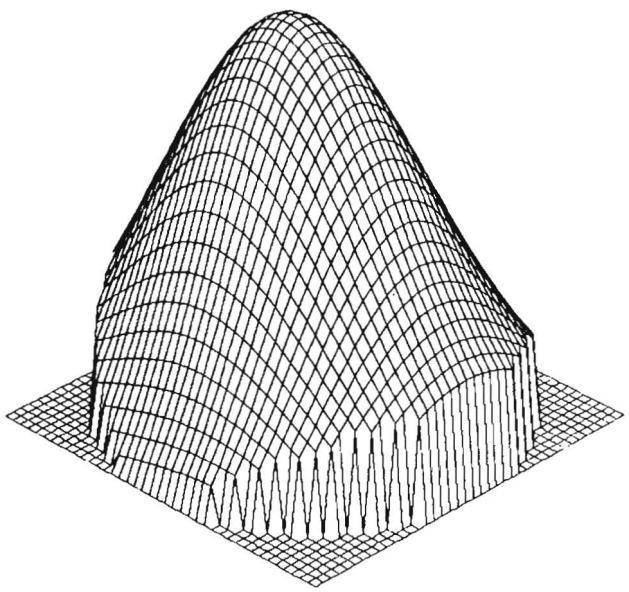

Fig. 7. The Main Horizontally Polarized Currents for a Pyramidal Horn, with TE10 + TE20 (Compensating) Modes.

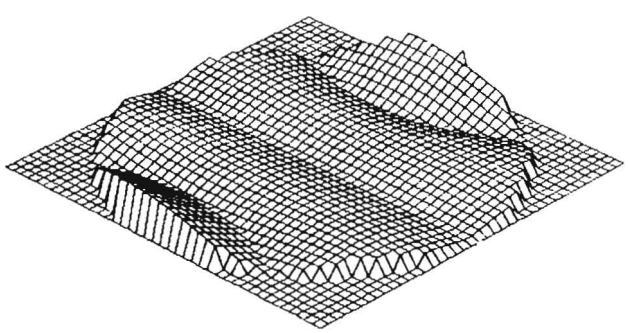

Fig. 8. The Minimized Cross-Polarized Currents, of −34 dB, For a Square Horn, with Horizontal Polarization.

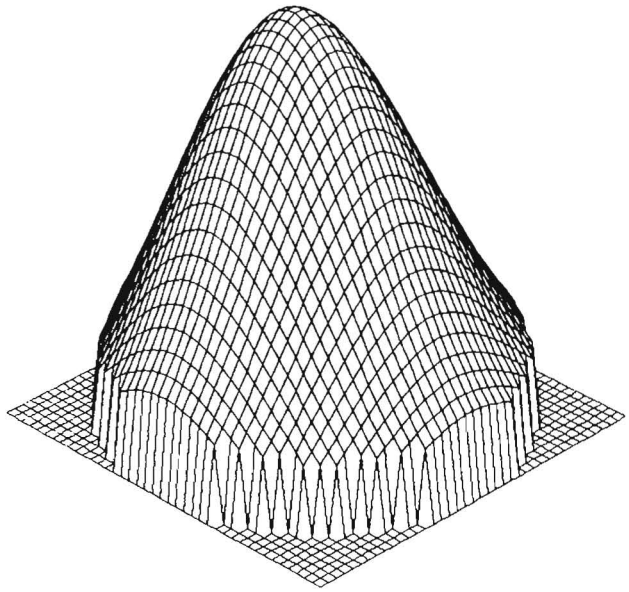

Fig. 9. The Main Polarized Currents for the Diagonal Horn, with the Fundamental Modes TE10 + TE01.

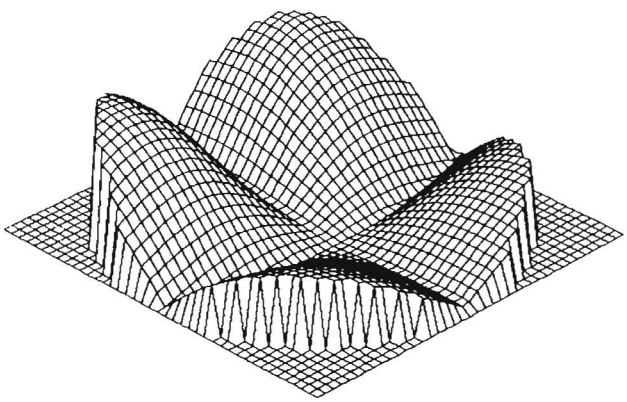

Fig. 10. The Cross-Polarized Currents for the Diagonal Horn, with the Fundamental Modes and Vertical Polarization.

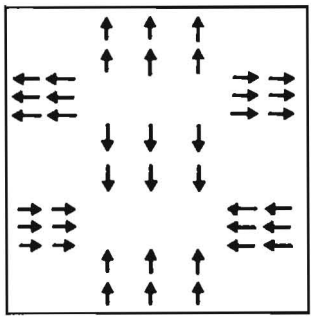

TM21 Mode.

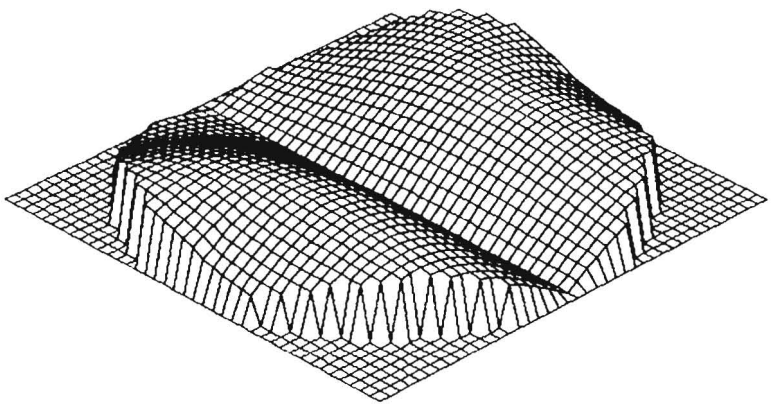

Fig. 11. The Cross-Polarized Currents for the Diagonal Horn, with Addition of the compensating Mode TM21, Which is shown above this figure, for vertical polarization.

Conclusions

1. The TE11 and the TE20 modes are the most succesful mix with the fundamental TE10 mode for control of the depolarized currents of offset reflector antennas, using rectangular feed horns.

2. The excitation methods for these modes need some care; especially as the TE11 mode controls the vertical polarization and the TE20 mode controls the horizontal polarization, with both polarizations in the same feed, in order to confirm the frequency reuse capability.

3. Diagonal feed horns yield symmetrical radiation, and consequently slightly higher efficiency, but their depolarization is excessive and difficult to control.

References

Afifi, M.S. (1984) Modern Telecommunication Systems and Multibeam Antennas, *2nd Nat. Radio Sci. Symp. (URSI) Proc.* Cairo, pp. 383-395.

A-Nasser, I.N. and **Afifi, M.S.** (1987) Multibeam Contiguous Coverage for Domestic Satellite Services for Saudi Arabia, *Arb Gulf J. Scient. Res., Math. Phys. Sci.*, **A5**(1): 111-119.

Chen, C.C., Franklin, C.E., Wong, W.C. and **Croswell, W.F.** (1980) CONUS Time Zone Coverage Contoured Beam Antenna, *IEEE Int. Ant. and Prop. Symp. Proc., U.S.A.*, **AP 3-4:** 85-88.

Clarricoats, B.J.B., Brown, R.C. and **Ramanujam, P.** (1987) Comparizon of Dual Reflector Antennas for Small Earth Stations, *IEE Int. Conf. on Ant. and Prop., ICAP 87,* Univ. of York, U.K., 30 March-2 April, pp. 125-128.

Nagi, M., Afifi, M.S. and **Samarkandy, M.,** (1987) Feed Design and Performance of an Offset Reflector of Small Earth Station, *ARABSAT Symp. Proc.*, Riyadh, 29 Sep.-1 Oct., pp. 396-406.

Silver, S. (1949) Microwave Antenna Theory and Design, Rad. Lab. Series No. 12, McGraw Hill Co. Inc., New York, pp. 134, 342 and 421.

Welti, G.R. (1982) Technology Goals for High-Capacity Communication Satellites, *33rd Cong of the Int. Astron. Fed.,* Paris, France, Sept. 27-Oct. 2.

(Received 11/01/1988;
in revised form 02/07/1988)

تقليل تيارات الاستقطاب المتعامدة للهوائيات العاكسة المائلة باستخدام أبواق تغذية هرمية ذات موجات متعددة الانتشار

مصطفى سيد عفيفي

قسم الكهرباء ـ كلية الهندسة ـ جامعة الملك سعود ـ ص. ب ٨٠٠ الرياض ١١٤٢١
المملكة العربية السعودية

يقدم هذا البحث تحليلاً لتوزيع التيارات على سطح الهوائيات العاكسة المائلة باستخدام أبواق مغذية هرمية ذات موجات متعددة الانتشار. وقد أمكن تقليل نسبة التيارات المتعامدة بانتقاء نسب خلط موجات انتشارية معينة.

فبخصوص الأبواق الهرمية مائلة الاستقطاب والتي تكون تيارات متماثلة القيمة حول مركز الهوائي العاكس ـ مما يزيد قليلاً من كفاءة الأداء ـ فإنها تسبب تيارات متعامدة قوية تبلغ حوالي ـ ١٦ ديسيبل ـ في تجمعات رباعية متداولة بالاستقطاب العمودي على سطح العاكس. ومعالجة هذه بالموجات المتعددة ليس بالأمر السهل. وقد استخدمت نسبة كبيرة من موجات TM21 لتقليل نسبة هذا الاستقطاب إلى ـ ٢٦ ديسيبل. ويصعب توليد هذه الموجة المعدلة في الأبواق الهرمية المائلة.

أما بالنسبة للاستقطاب الرأسي في الأبواق العادية فإنه يمكن باستخدام موجات TE10 مع نسبة خلط بسيطة من موجات TE11 تقليل التيارات المتعامدة إلى أقل من ـ ٤٠ ديسيبل. وبالنسبة للاستقطاب الأفقي فإنه يحتاج لنسبة صغيرة من موجات TE20 . وفي هذه الحالة يقل مستوى التيارات المتعامدة إلى ـ ٣٤ ديسيبل فقط، علماً بأن مستوى التيارات المتعامدة من موجات TE10 فقط ـ بدون خلط ـ يبلغ بحدود ـ ٢٦ ديسيبل.